An Experimental Test of Lepton Universality through Bethe-Heitler production of Lepton Pairs in Hall D at Jefferson Lab
A Letter of Intent to PAC 44

Reinhard Schumacher[1], Justin Stevens[2], Bill Briscoe[3], Igor Strakovsky[3], Mark Dalton*[4], Alexandre Deur[4], Howard Fenker[4], Doug Higinbotham[4], Mike McCaughan[4], Eric Pooser[4], Elton Smith[4], Benedikt Zihlmann[4], Georgios Vasileiadisa[5], and Rory Miskimen[6]

[1]Carnegie Mellon University, Pittsburgh, PA 15213, USA
[2]College of William & Mary, Williamsburg, VA 23186, USA
[3]George Washington University, Washington, DC 20052, USA
[4]Thomas Jefferson National Accelerator Facility, Newport News, VA 23606, USA
[5]University of Athens, Athens, Greece
[6]University of Massachusetts Amherst, Amherst, MA 01003, USA

June 5, 2016

Abstract

We propose a new experimental test of lepton universality to take place in Hall D at Jefferson Lab. The experiment will measure concurrently the Bethe-Heitler reactions, $\gamma p \to \mu^+\mu^- p$ and $\gamma p \to e^+e^- p$, as a function of t down to $t_{\mathrm{min}} \sim 4.4\times10^{-4}$. This will allow the proton electric form-factor to be separately measured using both electron and muon probes down to this very low momentum transfer. This would be only the second experiment to do precision muon scattering from a proton at low

momentum transfer, after the MUSE experiment, and this experiment would extend to significantly lower momentum transfer. Effects due to two-photon exchange are diminished in the Bethe-Heitler process since both charges scatter from the proton.

This experiment will require a new active hydrogen target in order to achieve its goals. This target is necessary in order to precisely measure the very low momentum transferred to the proton in a way that is identical for both the muon and electron final states. The baseline design of the target is a 1 m long transverse time-projection chamber (TPC) filled with 5 atmospheres of hydrogen gas. Such a target is feasible and is discussed in some detail in this proposal. The experiment would also rely on the new muon detector being built for the Charged Pion Polarizability experiment.

This proposal demonstrates that, assuming 100% acceptance and efficiency, data from 30 days of beam time would be able to confirm or refute, with high statistical significance, the hypothesis that the muon perceives a proton charge radius which is 0.04 fm smaller than that perceived by the electron. Detailed simulations are underway to determine the exact acceptance and efficiency in order to demonstrate that potential systematic effects can be controlled.

Contents

1 Introduction

The proton radius puzzle describes the fact that the proton charge radius, measured using different techniques, disagrees to high significance. The charge radius of the proton is a fundamental property of the proton and has been measured using two general techniques and two probes. In particular, extractions have been done for electron scattering from the proton, the Lamb shift in muonic hydrogen, and the Lamb shift in normal atomic hydrogen. To date, the proton radius has not been extracted in muon scattering from a proton, since existing data have too high a momentum transfer and large uncertainties.

While there are many possible explanations for the proton radius effect (including experimental error) there exists the intriguing possibility that it is due to a violation of lepton universality. That is, the muon appears to see a different proton radius because of some fundamental difference between the muon and the electron, other than the mass. This could be, for example, a new interaction or particle that couples to muons and electrons differently. The confirmation that muons do indeed perceive a different charge radius for the proton would be important evidence for physics beyond our current understanding.

The puzzle is now 5 years old and there is much that is being done to try to find a resolution of the discrepancy. New measurements of the Lamb shift hydrogen have been performed and the data analysis is underway. The existing electron scattering data is undergoing an extensive set of different analyses by different groups. The PRad Experiment is currently taking data in Hall B at Jefferson Lab. It aims to significantly improve the proton radius extracted through electron scattering by measuring to much lower momentum transfer and using simultaneous measurement of Moller scattering to do absolute normalization. The MUSE Experiment [1], has been approved at the Paul Scherrer Institute to do a simultaneous measurement of the proton radius through muon and electron scattering in the same experiment.

Here we propose to measure the proton form factor with muonic and electronic probes using Bethe-Heitler pair-production from a photon beam. These form factor measurements would share a common determination of the momentum transfer, t, allowing an identical extraction of the proton radius in both electron scattering and muon scattering separately, with systematics that are different to existing and other planned measurements. This comparison will test whether a violation in lepton universality is responsible for the apparently different size of the proton. This measurement is complementary to the existing efforts, allowing an independent test using a different technique and extending to lower momentum transfer.

This experiment requires an active hydrogen target—a combined hydrogen target and detector that can be used to detect very low energy protons recoiling in the scattering from high energy photons. Such a target will track very low momentum recoil protons continuously from the initial interaction until they are stopped by the gas, allowing the momentum to be determined from the distance traveled. This type of target is possible with a photon beam since there is no need to have any insensitive regions directly along the beam path, as would be the case with an electron beam to avoid Moller events.

Section 2 presents the motivation for this new experiment, describing the proton radius puzzle and the potential for a violation of lepton universality between electron and muons. Section 3 describes the experiment itself, including a possible design for a new active hydrogen target that would meet the required specifications and demonstrating that it is feasible, in Section 3.4, and an estimation of the luminosity and rates for the experiment, in Section 3.5. Section 4 describes the data analysis that will be followed and the expected results. Backgrounds that need to be taken into account are also discussed.

2 Motivation

2.1 Proton Radius Puzzle

There exists a large discrepancy between the charge radius of the proton extracted using different measurement techniques. In the most precise result, measurements of the Lamb shift in muonic hydrogen have determined a value of 0.84087 ± 0.00039 fm [2, 3] which is 4%, or 7σ from the CODATA value of 0.8775 ± 0.0051 fm [4]. The CODATA value is composed of Lamb shift measurements in atomic electronic hydrogen, giving a value of 0.8758 ± 0.0077 fm, and an analysis of ep elastic scattering data, giving 0.895 ± 0.018 fm [5].

The mean-square value of the radius is given by the slope of the electric form factor, G_E, in the limit of zero momentum transfer to the proton,

$$r_p^2 \equiv -6 \frac{dG_E}{dQ^2}\bigg|_{Q^2=0} \tag{1}$$

where $Q^2 = -q^2 = -t$ is the negative of the square of the four-momentum transferred to the proton. This definition of the radius is appropriate both for scattering and in the atomic energy levels.

Unfortunately, the proton radius extracted from electron scattering experiments shows a strong dependence on the method used to extrapolate from the low Q^2 data to the slope at $Q^2 = 0$. The difficulty is in simultaneously dealing with large absolute normalization uncertainties and the relatively unconstrained shape at small Q^2. Figure 1 shows the value of the radius extracted versus time for the various techniques. Recent re-analyses of *ep* scattering data (not shown in Fig. 1) have extracted values consistant with the muonic hydrogen result [6, 7]. These analyses use the $O(Q^2)$ Taylor expansion for G_E applied to the 1974 Saskatoon and 1980 Mainz data [6] and the 2010 MAMI data [7]. This approach has attracted some criticism [8]. However, even neglecting the ep scattering data still leaves a 4.4σ discrepancy between measurements of the Lamb shift in muonic and electronic hydrogen, Fig 2.

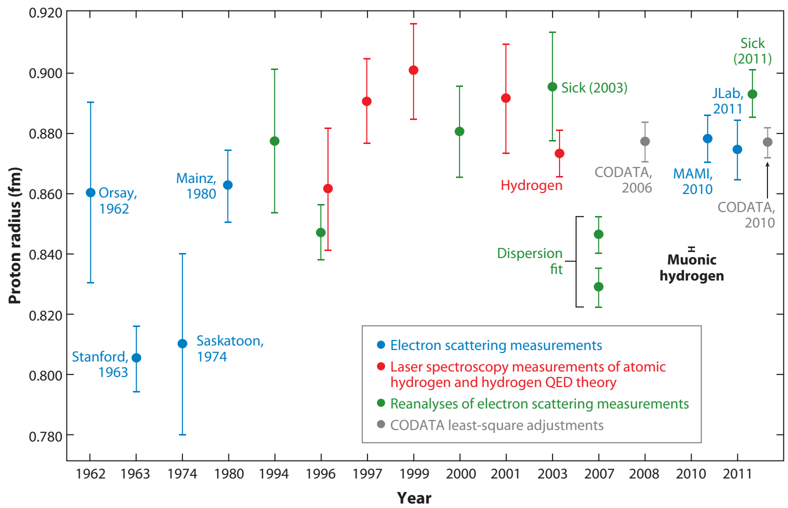

Figure 1: Proton radius determinations over time. Figure from Ref. [9]

The possible explanations for the radius puzzle are [9]: electronic hydrogen experiments are less accurate than stated; QED calculations are less accurate than stated; two-photon exchange due to proton polarizability is incorrect; or some physics, beyond the Standard Model (SM) of particle physics, causes the electron and the muon to have different interactions with the proton. Investigations into the puzzle surrounding this fundamental observable must continue.

2.2 Lepton Universality

There are tantalizing hints of a violation of lepton universality in existing data. The muon $g-2$ value is more than 3 standard deviations different from the SM expectation. As a percentage, this difference is small compared to the proton radius disagreement and fine tuning is needed in models to explain both. Importantly,

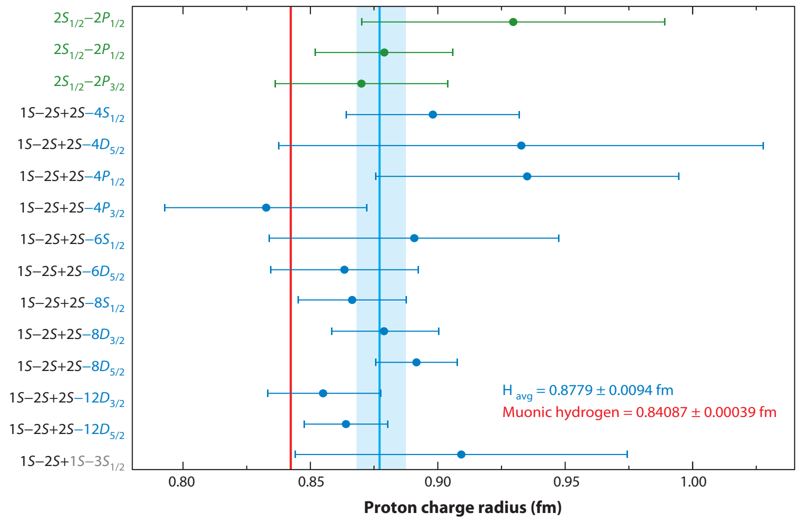

Figure 2: Proton radius extracted from transitions between various energy levels in atomic hydrogen compared to the result for muonic hydrogen, plotted in red with uncertainty. Taken together there is a 4.4σ discrepancy between the muonic and electronic radii. Figure from Ref. [9]

while the proton radius puzzle remains, the theoretical corrections to $(g-2)_\mu$ may be in doubt [10]. It has been difficult to construct models which explain the proton radius puzzle and the muon $g-2$ anomaly because lepton universality has been very well tested. Constraints from K-decay, measurements of the hyperfine splitting in muonium and muonic hydrogen, and the search for missing particles in Υ and J/ψ decays, amongst others, serve to limit the possible masses for new particles, with low masses favored [10].

There is now quite a significant difference from the Standard Model in semi-leptonic B decays, appearing to violate lepton universality. Three experiments have made measurements of the semi-leptonic decay of B mesons into D or D^* mesons. The BABAR experiment found that the ratios $\mathcal{R}(D) = \mathcal{B}(\overline{B} \to D\tau^-\overline{\nu}_\tau)/\mathcal{B}(\overline{B} \to D\ell^-\overline{\nu}_\ell)$ and $\mathcal{R}(D^*) = \mathcal{B}(\overline{B} \to D^*\tau^-\overline{\nu}_\tau)/\mathcal{B}(\overline{B} \to D^*\ell^-\overline{\nu}_\ell)$, where ℓ refers to either an electron or muon, exceed the Standard Model expectations by 2.0σ and 2.7σ, respectively. Taken together, this is a 3.4σ disagreement [11, 12]. The LHCb experiment has, to a certain extent, confirmed the BABAR result, measuring the ratio of branching fractions $\mathcal{B}(\bar{B}^0 \to D^{*+}\tau^-\bar{\nu}_\tau)$ and $\mathcal{B}(\bar{B}^0 \to D^{*+}\mu^-\bar{\nu}_\mu)$ to be 2.1σ greater than the SM expectation [13]. The BELLE experiment also pulls in the same direction [14]. The Heavy Flavor Averaging Group finds a combined difference from the Standard

Model, for all these results, of 3.9σ [15], summarized in Figure 3. In addition, The LHCb experiment has measured the branching fractions of the $B^+ \to K^+\mu^+\mu^-$ and $B^+ \to K^+e^+e^-$ and found the ratio to be 2.6 standard deviations from the SM value [16].

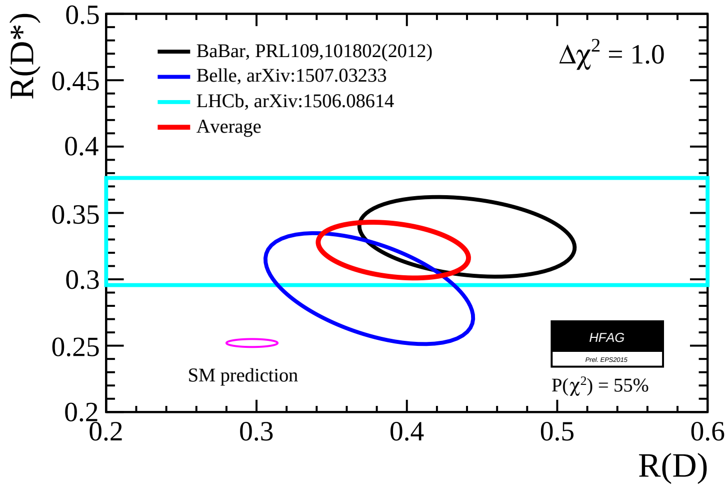

Figure 3: Measurements of the ratio of semi-leptonic B decay to different lepton flavors (see text.) The combined difference from the Standard Model is 3.9σ. Figure from the Heavy Flavor Averaging Group [15].

3 Description of Experiment

3.1 Introduction

The possibility that a violation in lepton universality is causing the proton radius puzzle can be directly tested by scattering muons and electrons from the proton in the same experiment. As mentioned previously, the MUSE experiment will perform direct scattering of separate muon and electron beams off the proton in the same experiment.

In this experiment, the proton form factor will be measured simultaneously using electronic and muonic probes, for $4.4\times10^{-4} < t < 0.3$, through the Bethe-Heitler process illustrated in Fig. 4. This will allow the direct comparison of the $\mu^+\mu^-$ production rate to the e^+e^- production rate, a test of lepton universality [17], and independent extraction of the proton radius for both muon and electron probes by, for example, using an analysis similar to those recently published [6, 7].

Both MUSE and Bethe-Heitler methods are attractive because measuring muons and electrons at the same time, in the same apparatus, allows a comparison that has many potential systematic effects cancel. The use of both methods will provide independent measurements of this important quantity with distinctly different systematic uncertainties. In contrast to the direct scattering method, the Bethe-Heitler production of lepton pairs from photons has a beam that is identical, and a measurement of the momentum transfer that is identical, for both processes. In addition, the experiment proposed here will extend to lower momentum transfer than the MUSE experiment.

3.2 Bethe-Heitler Process

The Bethe-Heitler pair-production process is depicted in Fig 4. The cross section for this process is given by

$$\frac{d\sigma^{\mathrm{BH}}}{dt dM_{ll}^2} = \frac{\alpha^3}{(s-M^2)^2} \frac{4\beta}{t^2(M_{ll}^2 - t)^4} \frac{1}{1+\tau} \times (C_E G_E^2 + C_M \tau G_M^2) \tag{2}$$

where M_{ll}^2 is the squared invariant mass of the lepton pair, $s = (\gamma + p)^2$ and $t = (p - p')^2$ are the Mandelstam invariants, M is the proton mass, $\alpha \equiv e^2/4\pi$, $\beta \equiv \sqrt{1 - 4m^2/M_{ll}^2}$ with m the lepton mass, and $\tau \equiv -t/4M^2$. C_E and C_M are complex kinematic coefficients given in Ref. [17]. G_E^2 and G_M^2 are the proton electric and magnetic form factors, allowing access to the charge radius through Equation 1.

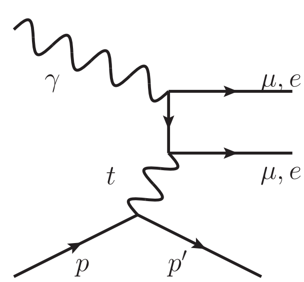

Figure 4: Feynman diagram for Bethe-Heitler pair production off a proton, t is the 4-momentum transferred to the proton, $-t = Q^2$ in electron scattering.

Figure 5 shows the Bethe-Heitler cross section for muons and electrons as a function of t for various M_{ll}^2. The cross section falls extremely rapidly with increasing momentum transfer. The lower the energy of protons that can be detected, the higher

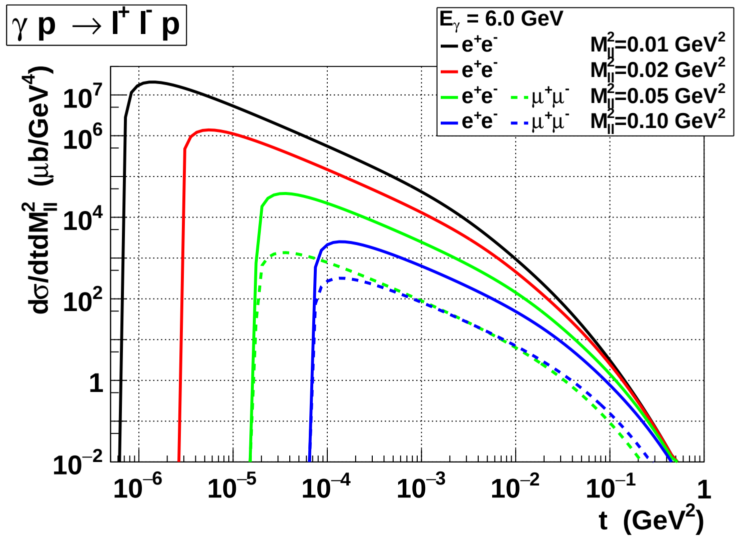

Figure 5: Curves to illustrate the cross section for the production of Bethe-Heitler pairs, differential in t and M_{ll}^2, for a photon beam of 6 GeV. Analytic expressions obtained from Ref. [17]. The kinematic minimum for the production of muon pairs is $M_{\mu\mu}^2 > 4.47 \times 10^{-2}$ GeV^2, while for electron pairs it is $M_{ee}^2 > 1.04 \times 10^{-6}$ GeV^2. The kinematic minimum in t depends on M_{ll}^2.

the rate of Bethe-Heitler pairs and the shorter the required beam time. Figure 6 shows the total Bethe-Heitler cross section as a function of the minimum observable proton momentum (the differential cross section of Fig. 5 has been integrated over all M_{ll}^2 and over t from a $t_{\rm min}$ which corresponds to the displayed $P_{\rm min}$).

3.3 Experimental Setup

We propose a simultaneous measurement of the production of e^+e^- and $\mu^+\mu^-$ pairs in Hall D at Jefferson Lab where there is a high energy photon beam and detector package optimized for high luminosity running. A tagged photon beam of the highest achievable brightness will be incident on a novel active hydrogen target, operated as a time-projection-chamber (TPC).The recoil proton will be detected down to low momentum using the active target.

There are 2 possibilities for the setup of the experiment. A *solenoid setup* is proposed, in which the active target would be placed in the location of the current GlueX target, within the bore of the solenoid magnet and the Bethe-Heitler leptons and scattered proton would be momentum analyzed in the solenoid field. A *dipole*

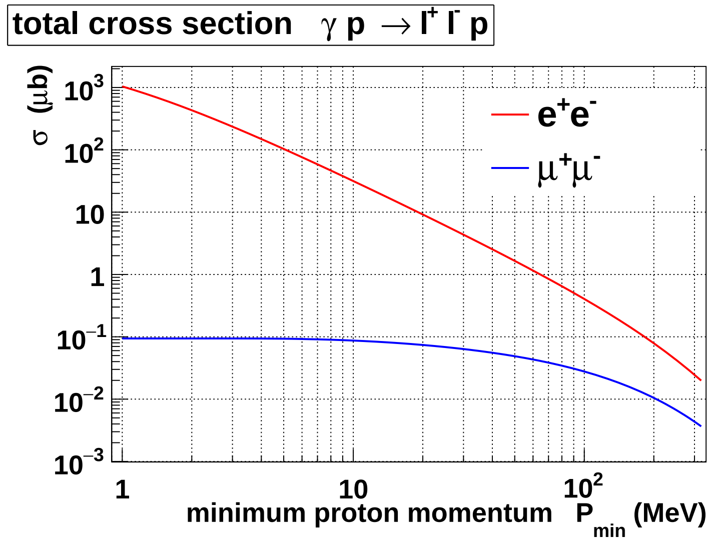

Figure 6: The total cross-section for Bethe-Heitler production of $\mu^+\mu^-$ and e^+e^- pairs as a function of the minimum proton momentum used in the integral, $P_{\rm min}$. The ability to detect lower momentum protons significantly increases the total cross-section for e^+e^- pairs, less so for $\mu^+\mu^-$ pairs.

setup is a potential backup, the active target could be placed within a new solenoid placed upstream of the pair-spectrometer dipole magnet. The protons would be analyzed by the solenoid and the leptons would be analyzed by the dipole.

The baseline design is the solenoid setup. Here the electron or muon pair will be tracked through the existing Forward Drift Chamber (FDC), Time Of Flight (TOF) and Forward Calorimeter (FCAL) detectors. Information on the existing apparatus in Hall D can be found in the GlueX proposal [18]. Electrons will be identified using E/P considerations in the FCAL. Muons will be identified using a new muon detector to be installed in Hall D, downstream of the FCAL, for the Charge Pion Polarizability (CPP) experiment [19]. Low momentum protons, up to $P \sim 56$ MeV/c, would be contained within the target. Higher momentum protons would be measured through curvature and in the surrounding Central Drift Chamber (CDC), with effectively no maximum detectable proton momentum. This uses existing equipment except for the active target and the new muon detector.

The dipole setup would provide higher acceptance and better resolution in the detection of the leptons but would require significant new equipment. The UVA solenoid magnet that will be used for the approved TDIS experiment would also be used for the target here. It is 1.5 m long, has a 40 cm bore and up to 4 Tesla field.

A 35 cm diameter target will fit within the magnet and will contain protons with momentum up to 80 MeV (equivalent to $-t = 0.0064$ GeV^2/c^2) and measure proton momentum up to 1.4 GeV/c through curvature.

In both cases, protons will be identified through their energy loss in the active target, which is approximately 50 times minimum ionizing. The detection of all the final state particles makes the reaction kinematically complete, allowing the conservation of 4 momentum to be used to improve resolution.

3.4 Active Hydrogen Target Design

The intention with a new active hydrogen target is to push the detection of the recoiling proton down to the very lowest possible values of momentum. Doing this decreases the length of extrapolation required to the zero momentum limit and increases statistics. This also helps with background since both inelastic interactions such as time-like Compton scattering and contributions from the proton magnetic form factor decrease with momentum transfer.

The lowest momentum spectator tagging system successfully implemented at JLab was for the BoNuS experiment, which studied quasi-free neutrons by selecting very low momentum spectator protons from a deuterium target. The apparatus was able to detect protons, down to 70 MeV/c, using a radial TPC [20]. A narrow kapton straw contained 7 atmospheres of deuterium gas. The target was surrounded by helium gas at atmosphere, and then by the TPC which had a thin entrance window and a drift gas of helium and dimethyl ether (DME) at atmosphere. Future JLab experiments, such as a higher energy version of BoNuS (BoNuS12) and Tagged Deep Inelastic Scattering (TDIS), will use similar tagging detectors to detect low energy protons and other nuclear fragment spectators. The precise geometry and design of these systems depend crucially on the physics of interest and on their eventual location. The BoNuS12 detector is very similar to BoNuS, and features a number of improvements, but will still have a limit of 70 MeV/c because the protons must still travel through the high-density target gas and windows before detection.

With an active target the minimum momentum is much lower because the whole volume is sensitive and the proton is detected from the initial interaction until the end of the track. The length of the track is used to determine the proton momentum down to the lowest momentum protons while curvature is used for higher momentum protons that escape the target.

Here we consider the solenoid setup where the active target is installed in the bore of the solenoid magnet. In this case it would likely be a cylindrical shape, to fit into the 18 cm diameter aperture of the Central Drift Chamber, with a length of up to 1 meter, in order to maximize rate. The length is limited by the desire to have a lepton pair that is created at the upstream end of the target, remain within the radius of the TPC and through the downstream face. The baseline design is a 1 meter long hydrogen TPC at 5 atmospheres of pressure, Figure 7. This gives a total areal density presented to the beam of 2.7×10^{22} cm^{-2}, which is about 50 times smaller that the 30 cm long liquid hydrogen target of GlueX.

The final design of this TPC will be a somewhat complex interplay between the various factors that influence the experiment which will have to be optimized with careful simulation. For example, an increase in the target and detector density would increase the experiment luminosity, but it would increase the cost and complexity of dealing with the high pressure vessel and also decrease the track length of a low momentum proton making it more difficult to detect and measure its momentum and possibly increasing the minimum accessible momentum. The luminosity can also be increased by increasing the length of the target but this directly increases the cost and difficulty of the project.

3.4.1 Feasibility

Hydrogen can be a difficult gas to use for gaseous detectors. It has a low breakdown voltage and does not "quench" ultraviolet photons which may be produced from avalanche processes during the gas amplification stage at GEM foils or anode wires. Such photons may travel a long distance and generate new charges interacting with metallic surfaces [21]. Hydrogen also has a low drift velocity [22], which is relevant at high rates.

Despite these difficulties, a number of hydrogen active-targets have been successfully operated. The IKAR TCP [23], developed in Gatchina, was used in the Coulomb interference experiments WA9 and NA8 at CERN [24]. The MAYA active target was used to study exotic beams interacting with light nuclear targets [25, 26]. Active targets were also used in a series of experiments studying muon catalyzed fusion (μCF) [27]. All of these targets operated in ionization mode without gas amplification.

The E612 experiment at Fermilab operated a 15 atmosphere hydrogen gas TPC, as an active target, in a high energy photon beam, $75 < E_\gamma < 148$ GeV, to measure the diffractive dissociation of photons on hydrogen [28, 22, 29]. They found that gains of $2 - 5 \times 10^4$ could be achieved, before the onset of self-sustained discharge, independent of pressure and sense wire diameter. In this target, the ionization was drifted in the axial (beam) direction and detected by a set of concentric octagonal sense wires.

The MuCap experiment has demonstrated the successful operation of an active-target TPC with gas amplification in ultra-prue hydrogen [30, 21]. They operated a Multi Wire Proportional Chamber (MWPC) at 10 atmospheres, demonstrating gas gains up to 5000, although it was routinely operated with a gain of 125. The sensitive volume was $(15 \times 12 \times 30)$ cm^3. The ionization was drifted downwards, transverse to the beam direction, where it was collected on wires with 4.0 mm wire spacing in the x and z directions, and timing resolution of 1.1 mm in the y direction. The drift field was produced with $\sim$ 30 kV and the gas amplification achieved with voltage $\sim$ 5.5 kV.

3.4.2 Transverse Drift Geometry

The most attractive design is a transverse-drift TPC, Fig 7. In this case, the drift distance will be about 11 cm, given by the width of the apparatus which has to fit into the CDC aperture.

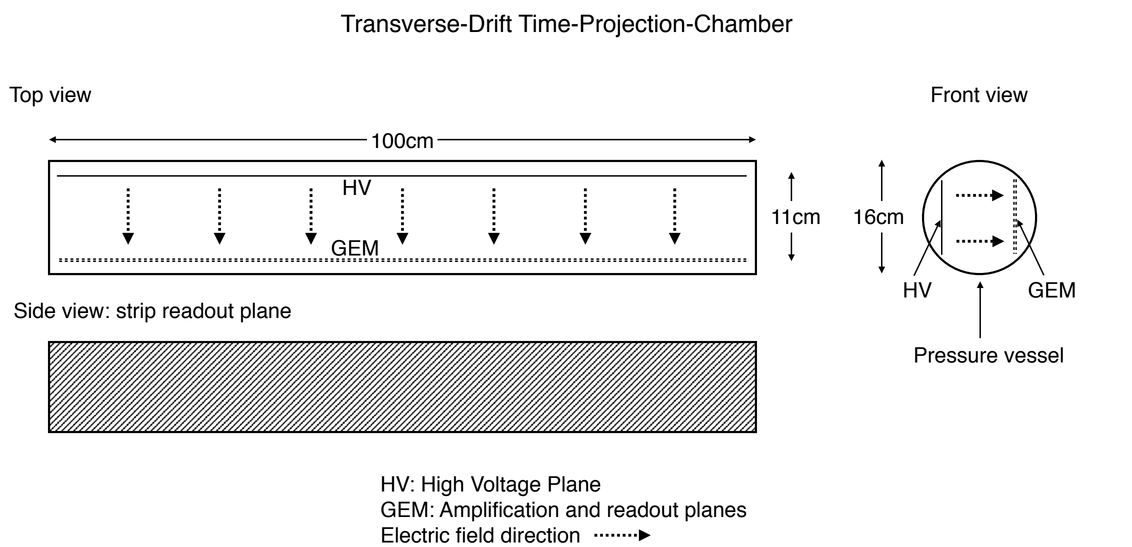

Figure 7: Schematic view of the proposed active target, baseline design.

This configuration, with a potential difference of 10 kV across a 11 cm drift distance, would give a small, but reasonable, reduced field $E/p \sim 0.24$ V/cm/torr at 5 atmospheres. The drift velocity for hydrogen at that reduced field is about 3.5×10^5 cm/s, from the parametrization of the TREAD group [29, 22], which agrees well with values calculated by the Magboltz and Garfield simulations [21]. This gives a typical drift time of 16 μs.

This design has a number of advantages compared to either radial or axial drift TPCs. The drift distance is necessarily short and allows the use of a relatively low voltage in order to drift the gas. The active target may be of arbitrary length. Since the charge does not drift along the beam, the potential for ambiguity is reduced.

The transverse drift design has a large surface area of readout that needs to be instrumented, requiring more readout channels. Due to the perpendicular electric and magnetic fields, the drift direction will have a Lorentz angle with respect to the electric field direction. This is expected to be manageable size and not significantly impact the size of the active area.

3.4.3 Readout and Resolution

The ionization left by the recoil protons will need to be amplified and read out. This could be done using 3 layers of gas electron multiplier (GEM) foils prior to being collected on a readout plane.

An attractive option for the electronics is the 64-channel, pipelined DREAM (Dead-timeless Readout Electronics ASIC for Micromegas) chip [31], which was designed for use in CLAS12. The chip collects the charge, amplifies and filters it, then discriminates the pulse and stores the analog signal in a buffer. If a readout is triggered, the sampled signals are read-out asynchronously without stopping the analog storage process allowing "deadtime free" operation.

Two effects that limit the resolution when using the range to determine the momentum are straggling and diffusion. The straggling, or statistical variation in range for particles of the same energy, is relatively small for protons propagating through 5 atmospheres of hydrogen gas. The straggling distributions were determined using SRIM [32] and found to change from 30 μm for 1 mm tracks to 550 μm for 5 cm tracks. Diffusion is a little more difficult to estimate. The TREAD group found diffusion in hydrogen gas at 15 atmospheres started at about 120 μm and increased slowly with drift distance as 22 $\mu\text{m}\cdot\text{cm}^{-\frac{1}{2}}$ [22]. The intrinsic resolution for millimeter length tracks is thus below 200 μm.

In this device we will therefore aim for a resolution in the readout of 200 μm using a strip readout. A pair of stereoscopic strip planes, with a strip pitch of 0.2 mm, oriented at 45 degrees to the vertical, would require about 10,000 channels to instrument. BoNuS12 plans to use a pixel readout with 2.5×4 mm pixels arranged with 100 pixels in Z, and 200 pixels around the azimuth. These 20,000 channels would have a significantly coarser resolution, but are required to deal with their greater rate [33]. Considering the low rates, if necessary the number of channels could be reduced using a multiplexing technique. With a drift velocity of 3.5×10^5 cm/s obtaining 200 μm resolution in the drift direction will require timing resolution of 57 ns. This is attainable using the DREAM chip, which has a minimum sampling period of 50 ns. Achieving 200 μm resolution will allow observation of proton tracks that are 2 mm long.

Using SRIM or the National Institute of Standards and Technology's PSTAR program [34], which calculate stopping power and range tables for protons in various materials, a 2 mm track corresponds to a proton of 21 MeV/c.

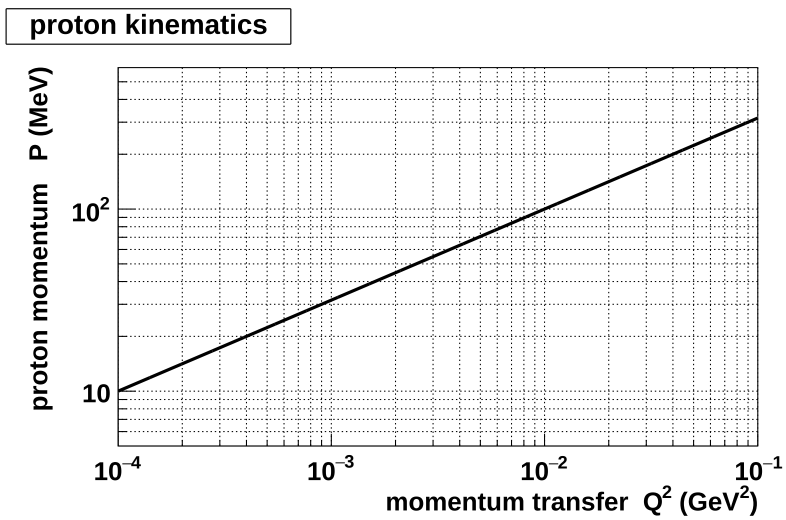

Figure 8: Relationship between the magnitude of the 4-momentum transferred to a proton at rest and the magnitude of its resulting momentum.

The 4-momentum transferred to the proton, t, is directly related to the magnitude of the proton 3-momentum through $P = \sqrt{(M_p - \frac{t}{2M_p})^2 - M_p^2}$. Figure 8 gives a graphical representation of this relationship. The 21 MeV/c momentum corresponds to a 4-momentum transfer of 4.4×10^{-4} GeV^2/c^2. Table 1 shows the minimum 4-momentum achievable in various experiments.

3.5 Luminosity and Rates

The photon beam is produced by coherent bremsstrahlung on a thin diamond wafer. The diamond has its lattice carefully oriented with respect to the beam direction in order to enhance the production of photons at a particular energy. This procedure produces a peak of photons that are linearly polarized, the coherent part, and a continuum of unpolarized photons with the usual bremsstrahlung $1/E$ spectrum, see

Experiment	year	t_{min} ($\times 10^{-3}$ GeV^2/c^2)	P_{min} (MeV/c)	Reference
MAMI	2010	3.8	62	Ref.[35]
Mainz	1980	5.1	71	Ref.[36]
Saskatoon	1974	5.8	76	Ref.[37]
MUSE	—	1.5	39	Ref.[1]
PRad	—	0.2	13	Ref.[38]
This proposal	—	0.44	21	Sec. 3.4

Table 1: The t_{min}, and corresponding P_{min}, achieved or expected for existing and future scattering measurements of the proton radius.

Fig. 9a) for example. The coherent photons have a narrower angular spread than the incoherent photons and thus they may be enriched through collimation. The energy of each photon may be deduced by detecting the electron that radiated it. The production of the photons is done in a separate experimental hall, 75 m upstream of Hall D, giving the photons a long distance to travel to aid in the collimation. The electron beam is bent in the Tagger Magnet before entering the beam dump—electrons that have lost energy to photon radiation are bent more and impact detectors to the side of the magnet.

The limit to the flux of tagged photons in Hall D is the ability of the tagger detectors to handle the rate of scattered electrons in order to tag the beam. The tagger is instrumented with a high granularity tagging detector, called the Microscope, which captures the rate in the coherent peak, and lower granularity hodoscopes outside of this region.

The Microscope is believed to be able to handle an electron rate of 500 MHz before the rate induces gain sagging and pileup. If the photon beam is collimated before reaching the target this decreases the photons available for the experiment. The number of available photons can be increased by increasing the size of the collimator hole or by lowering the energy of the coherent peak, which enriches the coherent fraction of the beam and increases the fraction passing the collimator. Changing the energy of the coherent photons is achieved by reorienting the diamond radiator and moving the Microscope to the appropriate position along the tagger magnet. Lowering the energy of the coherent photons increases the efficiency of the coherent production mechanism, boosting the number of coherent photons compared to incoherent photons significantly and increasing the linear polarization of the beam. Increasing the collimator diameter increases the number of photons that make it to the experiment. Figure 9 shows the spectrum of photons at the target with the radiator set to produce

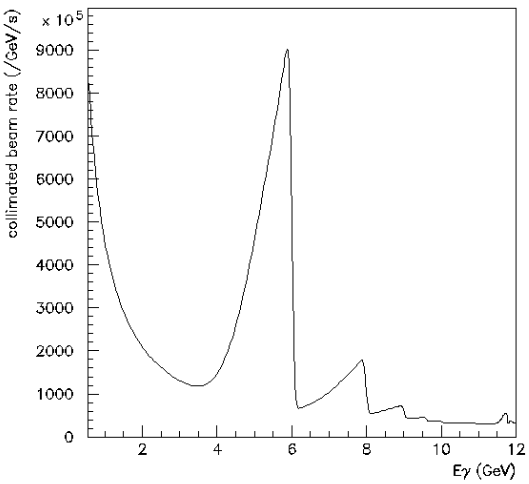

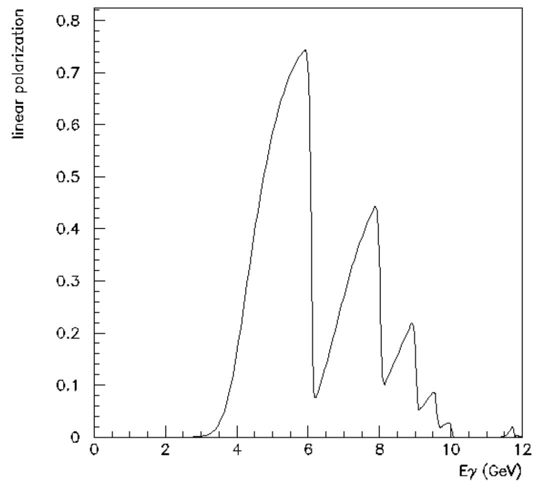

(a) The spectrum of photons that make it to the target.

(b) The average linear polarization of photons that make it to the target.

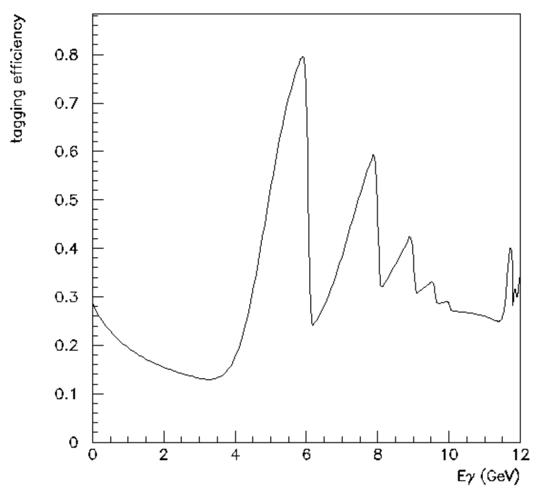

(c) The fraction of produced photons that make it to the target

Figure 9: Expectations for a photon beam from 500 nA of electron beam, a 20 μm thick oriented diamond and the 5 mm collimator [39].

6 GeV coherent photons and the 5 mm collimator in position [39].

The 500 MHz microscope rate, with a 6 GeV coherent peak, would be achieved with 500 nA of beam and a 20 μm thick diamond. Using the 5 mm collimator, there is a 60% probability that photons in the coherent part will make it to the experiment, a 300 MHz photon rate in the peak. The average polarization of this part of the beam would be $> 60\%$. In addition, another 100 MHz of tagged photons between 6 GeV and the endpoint at 12 GeV should make it to the target in this configuration. This allows a total tagged photon rate of 400 MHz.

Given the baseline target thickness, 2.7×10^{22} cm^{-2} (Sec. 3.4), and 400 MHz beam, this gives a luminosity of 1.1×10^{-2} nb^{-1}s^{-1}. A data taking period of 30 days in such a configuration would give an integrated luminosity of 2.8×10^4 nb^{-1}. Using a total cross sections of $\sigma_{\mu\mu} = 53$ nb and $\sigma_{ee} = 8.2$ μb, corresponding to $P_{\rm min}$ = 21 MeV/c in Figure 6, gives 1.8 million $\mu^+\mu^-$ pair events and 82 million e^+e^- pair events. This does not include effects due to finite acceptance and efficiency of the detectors, which would need to be simulated using a model of the full detector.

The total cross section for production of hadrons with multi-GeV photons is ~ 120 μb [40], which gives a rate of 1.3 kHz. The total Bethe-Heitler cross section for e^+e^- pair production of $\sim$13 mb gives a rate of 140 kHz. This is the signal of this experiment, but the majority of this rate will not be accessible to the active target since the protons will have too little energy to leave appreciable ionization in the gas and the e^+e^- pairs themselves will leave only lightly ionizing tracks. The rate of ionized tracks with dE/dX corresponding to a proton is thus quite low. See Sec. 3.5 for a discussion of the luminosity used to get these rates. With a rate of 140 kHz and the average drift time of 16 μs there are an average of 2.2 tracks drifting simultaneously within the target.

4 Expected Results

4.1 Analysis Strategy

In this experiment the best analysis seems to be to determine the proton radius separately for e^+e^- and $\mu^+\mu^-$ production and then compare them. In this way the most systematic benefit is obtained. Others have proposed a different experimental strategy that requires only detection of the proton, but it turns out to be quite difficult to achieve the same precision with this strategy. This is discussed in more detail below.

4.1.1 Proton only rate comparison

This strategy was proposed in Ref. [17], where it is discussed in some detail. The idea is to make the measurement by detecting only the proton. Detecting the proton momentum and polar lab angle allows both t and M_{ll}^2 to be determined, assuming that you know that a Bethe-Heitler event took place. Other processes can be avoided by restricting the analysis to a region between π^0 production at $M_{ll}^2 \sim 0.018$ GeV^2/c^2 and the $\pi\pi$ production threshold at $M_{ll}^2 \sim 0.078$ GeV^2/c^2. The $\mu^+\mu^-$ production threshold occurs within this range at $M_{ll}^2 \sim 0.045$ GeV^2/c^2. The analysis then proceeds by comparing the e^+e^- rate in the low region $0.018 < M_{ll}^2 < 0.045$ to the $e^+e^- + \mu^+\mu^-$ rate in a high region $0.045 < M_{ll}^2 < 0.078$ in bins of t.

The advantages of this strategy are that Bethe-Heitler events in which both of the leptons travel down the beam pipe can still be analyzed, which increases statistics. In fact, no lepton detection is required but directly detecting some of the lepton pairs would be desirable since it allows verification of the technique for fully reconstructed events. The proton angle would need to be reconstructed to sufficient precision to determine M_{ll}^2 well but this should not present major difficulty.

This strategy has the significant additional challenge of needing an experimental trigger that recognizes the proton recoil events of interest using signals only from the proton target itself. This would be quite a demanding requirement on the active target readout electronics and trigger system.

The analysis inflates the uncertainty because it relies on subtracting one large number from another. Given that the e^+e^- cross section is about 10 times larger than the $\mu^+\mu^-$ cross section—a determination of $\sigma(e^+e^-)$ and $\sigma(e^+e^- + \mu^+\mu^-)$, both to a statistical precision of 1% would lead to statistical precision of about 15% on $R_{\mu/e} \equiv \frac{\sigma(e^+e^-+\mu^+\mu^-)}{\sigma(e^+e^-)} - 1$, the most useful quantity for comparison to theory. The size of the proton radius effect on $R_{\mu/e}$ is 2% at $-t = 0.02$ GeV^2/c^2 Ref. [17], which therefore requires a precision of 0.013% on $\sigma(e^+e^-)$ and $\sigma(e^+e^- + \mu^+\mu^-)$ to make a 5σ measurement.

Thus it can be seen that this strategy is extremely challenging.

4.1.2 Proton radius comparison

In this strategy, the proton radius is separately determined for e^+e^- and $\mu^+\mu^-$ production and the two radii are then compared. It requires the separate detection of e^+e^- and $\mu^+\mu^-$ pairs along with the detection of the proton. The experiment would be triggered on the leptons.

Precise normalization of the cross section is not required, since only the slope of the form-factor is relevant and an overall scale factor can be applied in the fit.

Determining the t-slope correctly does require an acceptance and efficiency that is constant as a function of t (or changes in a well known way), but only for each lepton species separately. It is not required that the apparatus has the same acceptance and efficiency for e^+e^- as for $\mu^+\mu^-$. This can be achieved by restricting the kinematics such that the data for each bin in t has the same detection region.

This approach is attractive as it will be only the second determination of the proton radius using a muon probe and would extend to significantly lower momentum transfer than the MUSE experiment, thus decreasing the extent of extrapolation required. The radius is extracted by doing a fit to the data, but there is currently some debate on the best procedure for doing this [6, 7, 8]. In terms of extracting the radius itself, the analysis will follow the best practices in the literature at the time the analysis is done. However, since the aim of the experiment is primarily to compare muons and electrons, it should be sufficient to apply the same procedure to both.

Figure 10 shows the statistical error on the e^+e^- and $\mu^+\mu^-$ pairs, with the same bins, compared to the potential size of the proton radius discrepancy, given the baseline design of 30 days of 400 MHz photons, a 1 m long, 5 atmosphere hydrogen-target, and 100% experimental acceptance and efficiency. The difference in cross section, from a violation of lepton universality, cannot be determined in a model independent way, so it is convenient to use the two different measured proton radii to estimate the size of the effect. A linear approximation to the form factor, $G_E = 1 - Q^2r^2/6$, is used to estimate the cross section for two proton radii, 0.88 fm and 0.84 fm. The ratio of the cross section for the two radii gives the size of the potential effect—by $-t \sim 0,015$ GeV^2/c^2 it is 1%. Care is needed in the interpretation since this linear approximation is only appropriate at low momentum transfer. The binning in t in the figures is such that no bin width corresponds to a difference of proton range that is less than 1 mm. Figure 11 shows the expected statistical uncertainties from MUSE, for comparison.

A linear fit to the e^+e^- data in Figure 10(a) is able to distinguish between a proton radius of 0.88 fm and 0.84 fm to extremely high significance (30σ), considering only data with $-t < 0.03$ GeV^2/c^2. Due to the decreased statistics, a linear fit to $\mu^+\mu^-$ data in Figure 10(b), in the same t range, has only a 5σ sensitivity. Extending the fit to $-t < 0.06$ GeV^2/c^2 would improve this significance to more than 10σ. The ultimate precision of this approach depends on the details of the extraction. This technique is therefore able to confirm or refute the hypothesis that the muon perceives a proton charge radius which is 0.04 fm smaller than that perceived by the electron.

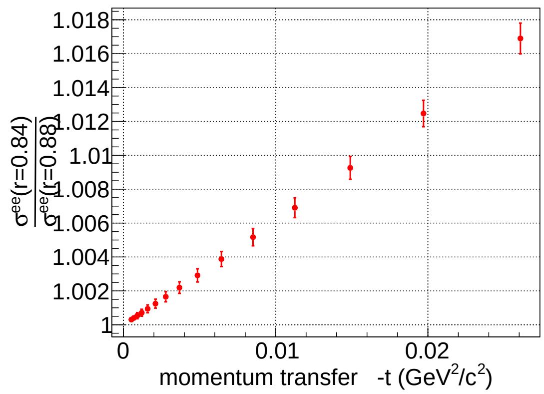

(a) Plot of the statistical uncertainties in the Bethe-Heitler production of e^+e^- pairs.

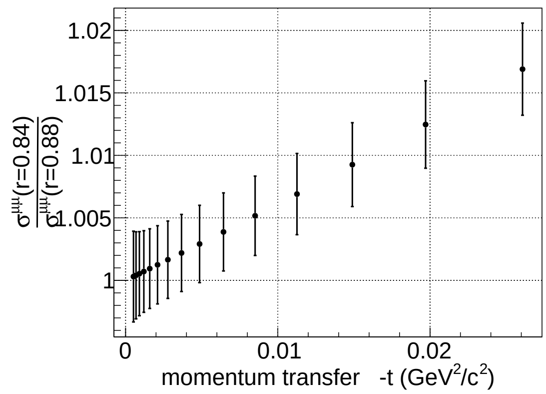

(b) Plot of the statistical uncertainties in the Bethe-Heitler production of $\mu^+\mu^-$ pairs.

Figure 10: These plots attempt to show the sensitivity of the experiment by comparing the statistical uncertainties with a naive estimate of the size of the potential effect. The points are shown with a central value that represents the ratio in cross section between a proton with radius 0.88 fm and a proton with radius 0.84 fm. This is purely illustrative since the linear approximation cannot be expected to extend beyond $-t > 0.02$ GeV^2/c^2.

4.2 Backgrounds

4.2.1 Production of $\pi^+\pi^-$

Pion backgrounds can be of concern since pions and muons have similar mass and, at the energies of interest here, are both minimally ionizing and therefore behave similarly in most detectors. In addition, pions decay almost exclusively to muons. The most notable sources of $\pi^+\pi^-$ pairs are from the decay of the ρ^0 (770) and from Primakov production. The total cross section for ρ^0 production is 10 μb, which is significantly larger that the Bethe-Heitler muon cross section of interest in this experiment.

This background can be rejected on an event by event basis using a combination of the muon detector and kinematics. If all 4% of the pions that decay before the detector are tagged as muons in the muon detector, this would give a pion contamination in the muon yield of 0.03% [19]. The invariant mass of the ρ^0 is significantly higher than the Bethe-Heitler pairs of interest, a cut on M_{ll}^2 would also remove almost all of the ρ^0 contribution.

The polarization of the beam will further help to check for and eliminate pions

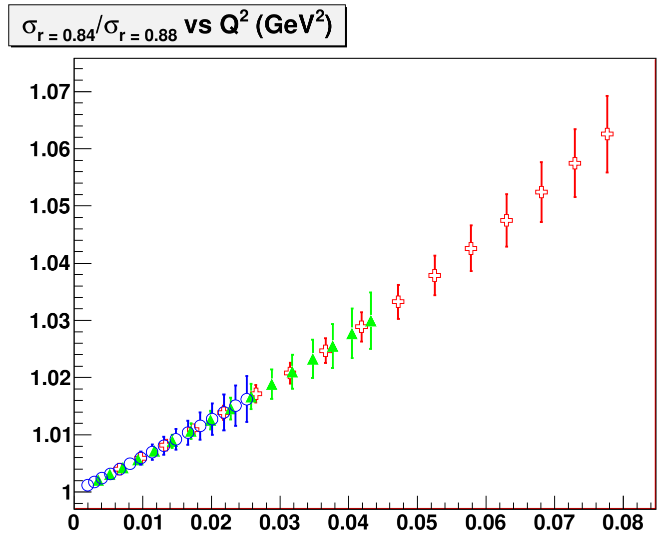

Figure 11: Figure from the MUSE proposal for μp elastic scattering [1]. Each color represents 30 days of beam at 210 MeV/c (Squares), 153 MeV/c (triangles) and 115 MeV/c (circles).

from both of these sources. The ρ^0 is produced with almost complete s-channel helicity conservation meaning that in the helicity frame there is an azimuthal dependence with the same magnitude as the photon polarization. Thus, any residual contamination in the $\mu^+\mu^-$ signal from ρ^0 could be detected by observing azimuthal modulation in the helicity frame. Primakov $\pi^+\pi^-$ and Bethe-Heitler $\mu^+\mu^-$ are produced with opposite sign azimuthal dependence in the lab frame. This serves as a handle on any remaining Primakov $\pi^+\pi^-$ events in the signal [19].

Given the proposed luminosity, this experiment would produce > 250 million ρ^0 particles, which will allow for a very precise measurement of the degree of s-channel helicity conservation in ρ^0 production down to very low t.

4.2.2 Irreducible backgrounds

Timelike Compton Scattering (TCS) is the photo-production of a heavy, timelike photon, which decays into a lepton pair. It is indistinguishable from Bethe-Heitler pair production but has a much smaller cross section. The cross section is difficult to calculate because it relies on detailed knowledge of the proton structure. Existing calculations show that even for a large $M_{ll}^2 = 5$ GeV^2/c^2 and requiring $\theta > \pi/4$ in order to emphasize the TCS contribution, the Bethe-Heitler cross section is still more than 10 times larger than for TCS [41]. The interference between TCS and the Bether-Heitler process is estimated to be only a 0.07% effect on the ratio of $\mu^+\mu^-$ pairs to e^+e^- pairs at $E_\gamma = 500$ MeV and $-t = 0.2$ GeV^2/c^2 [17]. Calculations based on Generalized Parton Distributions will be needed to estimate the contribution at the specific kinematics of interest to this proposal.

Existing elastic electron-scattering data is subject to the effect of 2γ exchange, where the proton may be excited internally, which affects the scattering cross section. While this is not expected to be large on the scale of the proton radius difference, these effects are not quantitatively understood yet. The MUSE experiment will provide data on this since it will measure scattering with positive and negative charged beam particles, where the 2γ effects enter with opposite sign. Since the Bethe-Heitler reaction in this proposal produces lepton pairs, which contain both charge states, either of which could have interacted with the proton, the sensitivity to potential effects from 2γ exchange with the nucleus are diminished. The Bethe-Heitler reaction requires different QED radiative corrections to those routinely applied to lepton scattering. It is expected that calculations of these QED radiative corrections specific to Bethe-Heitler will be necessary before interpreting the data.

5 Summary

This proposal demonstrates that a simultaneous measurement of Bethe-Heitler production of e^+e^- and $\mu^+\mu^-$ pairs could make an important contribution towards resolving the proton radius puzzle. A confirmation that the effect is indeed caused by a violation of lepton universality would be of high impact and would help guide searches for the new physics responsible. Alternatively, determining that the leptons see the same proton radius would be a less exciting but no less valuable resolution.

References

[1] R. Gilman *et al.*, "A Proposal for the Paul Scherrer Institute M1 beam line Studying the Proton Radius Puzzle with p Elastic Scattering The MUon proton Scattering Experiment (MUSE) Collaboration,". http://www.physics.rutgers.edu/~rgilman/elasticmup/muse_prop_2012.pdf.

[2] R. Pohl *et al.*, "The size of the proton," *Nature* **466** (2010) 213–216.

[3] A. Antognini *et al.*, "Proton Structure from the Measurement of $2S - 2P$ Transition Frequencies of Muonic Hydrogen," *Science* **339** (2013) 417–420.

[4] P. J. Mohr, B. N. Taylor, and D. B. Newell, "CODATA Recommended Values of the Fundamental Physical Constants: 2010," *Rev. Mod. Phys.* **84** (2012) 1527–1605, arXiv:1203.5425 [physics.atom-ph].

[5] I. Sick, "On the RMS radius of the proton," *Phys. Lett.* **B576** (2003) 62–67, arXiv:nucl-ex/0310008 [nucl-ex].

[6] D. W. Higinbotham, A. A. Kabir, V. Lin, D. Meekins, B. Norum, and B. Sawatzky, "The Proton Radius from Electron Scattering Data," arXiv:1510.01293 [nucl-ex].

[7] K. Griffioen, C. Carlson, and S. Maddox, "Are Electron Scattering Data Consistent with a Small Proton Radius?," arXiv:1509.06676 [nucl-ex].

[8] M. O. Distler, T. Walcher, and J. C. Bernauer, "Solution of the proton radius puzzle? Low momentum transfer electron scattering data are not enough," arXiv:1511.00479 [nucl-ex].

[9] R. Pohl, R. Gilman, G. A. Miller, and K. Pachucki, "Muonic hydrogen and the proton radius puzzle," *Ann. Rev. Nucl. Part. Sci.* **63** (2013) 175–204, arXiv:1301.0905 [physics.atom-ph].

[10] C. E. Carlson, "The Proton Radius Puzzle," *Prog. Part. Nucl. Phys.* **82** (2015) 59–77, arXiv:1502.05314 [hep-ph].

[11] **BaBar** Collaboration, J. P. Lees *et al.*, "Evidence for an excess of $\bar{B} \to D^{(*)}\tau^-\bar{\nu}_\tau$ decays," *Phys. Rev. Lett.* **109** (2012) 101802, arXiv:1205.5442 [hep-ex].

[12] **BaBar** Collaboration, J. P. Lees *et al.*, "Measurement of an Excess of $\bar{B} \to D^{(*)}\tau^-\bar{\nu}_\tau$ Decays and Implications for Charged Higgs Bosons," *Phys. Rev.* **D88** no. 7, (2013) 072012, arXiv:1303.0571 [hep-ex].

[13] **LHCb** Collaboration, R. Aaij *et al.*, "Measurement of the ratio of branching fractions $\mathcal{B}(\bar{B}^0 \to D^{*+}\tau^-\bar{\nu}_\tau)/\mathcal{B}(\bar{B}^0 \to D^{*+}\mu^-\bar{\nu}_\mu)$," *Phys. Rev. Lett.* **115** no. 11, (2015) 111803, arXiv:1506.08614 [hep-ex]. [Addendum: Phys. Rev. Lett.115,no.15,159901(2015)].

[14] **Belle** Collaboration, M. Huschle *et al.*, "Measurement of the branching ratio of $\bar{B} \to D^{(*)}\tau^-\bar{\nu}_\tau$ relative to $\bar{B} \to D^{(*)}\ell^-\bar{\nu}_\ell$ decays with hadronic tagging at Belle," *Phys. Rev.* **D92** no. 7, (2015) 072014, arXiv:1507.03233 [hep-ex].

[15] **Heavy Flavor Averaging Group** Collaboration, "Average of R(D) and R(D*) for EPS-HEP 2015,". http://www.slac.stanford.edu/xorg/hfag/semi/eps15/eps15_dtaunu.html.

[16] **LHCb** Collaboration, R. Aaij *et al.*, "Test of lepton universality using $B^+ \to K^+\ell^+\ell^-$ decays," *Phys. Rev. Lett.* **113** (2014) 151601, arXiv:1406.6482 [hep-ex].

[17] V. Pauk and M. Vanderhaeghen, "Lepton universality test in the photoproduction of e^-e^+ versus $\mu^-\mu^+$ pairs on a proton target," arXiv:1503.01362 [hep-ph].

[18] **GlueX** Collaboration, "Mapping the Spectrum of Light Quark Mesons and Gluonic Excitations with Linearly Polarized Photons,". http://www.jlab.org/exp_prog/proposals/06/PR12-06-102.pdf.

[19] R. Miskimen *et al.*, "Measuring the Charged Pion Polarizability in the $\gamma\gamma \to \pi^+\pi^-$ Reaction,". www.jlab.org/exp_prog/proposals/13/PR12-13-008.pdf.

[20] H. C. Fenker *et al.*, "BoNuS: Development and Use of a Radial TPC using Cylindrical GEMs," *Nucl. Instrum. Meth.* **A592** (2008) 273–286.

[21] J. Egger *et al.*, "A high-pressure hydrogen time projection chamber for the MuCap experiment," *Eur. Phys. J.* **A50** no. 10, (2014) 163, arXiv:1405.2853 [physics.ins-det].

[22] T. J. Chapin, R. L. Cool, K. A. Goulianos, K. A. Jenkins, J. P. Silverman, G. R. Snow, H. Sticker, S. N. White, and Y.-H. Chou, "PERFORMANCE OF A HIGH PRESSURE HYDROGEN TPC," *Nucl. Instrum. Meth.* **A225** (1984) 550–556.

[23] A. A. Vorobyov, G. A. Korolev, V. A. Schegelsky, G. Ye. Solyakin, G. L. Sokolov, and Yu. K. Zalite, "A method for studies of small-angle hadron-proton elastic scattering in the coulomb interference region," *Nucl. Instrum. Meth.* **119** (1974) 509–519.

[24] J. P. Burq *et al.*, "Soft $\pi^- p$ and pp Elastic Scattering in the Energy Range 30-GeV to 345-GeV," *Nucl. Phys.* **B217** (1983) 285.

[25] C. E. Demonchy *et al.*, "First results of the new active target MAYA," *J. Phys.* **G31** (2005) S1831–S1835.

[26] C. Demonchy, W. Mittig, H. Savajols, P. Roussel-Chomaz, M. Chartier, B. Jurado, L. Giot, D. Cortina-Gil, M. Caamao, G. Ter-Arkopian, A. Fomichev, A. Rodin, M. Golovkov, S. Stepantsov, A. Gillibert, E. Pollacco, A. Obertelli, and H. Wang, "Maya, a gaseous active target," *Nuclear Instruments and Methods in Physics Research Section A: Accelerators, Spectrometers, Detectors and Associated Equipment* **573** no. 12, (2007) 145 – 148. `http://www.sciencedirect.com/science/article/pii/S0168900206022558`. Proceedings of the 7th International Conference on Position-Sensitive DetectorsPSD-77th International Conference on Position-Sensitive Detectors.

[27] D. Balin, V. Ganzha, S. Kozlov, E. Maev, G. Petrov, M. Soroka, G. Schapkin, G. Semenchuk, V. Trofimov, A. Vasiliev, A. Vorobyov, N. Voropaev, C. Petitjean, B. Gartner, B. Lauss, J. Marton, J. Zmeskal, T. Case, K. Crowe, P. Kammel, F. Hartmann, and M. Faifman, "High precision study of muon catalyzed fusion in d2 and hd gas," *Physics of Particles and Nuclei* **42** no. 2, (2011) 185–214. `http://dx.doi.org/10.1134/S106377961102002X`.

[28] T. J. Chapin, R. L. Cool, K. A. Goulianos, K. A. Jenkins, J. P. Silverman, G. R. Snow, H. Sticker, S. N. White, and Y.-H. Chou, "DIFFRACTION DISSOCIATION OF PHOTONS ON HYDROGEN," *Phys. Rev.* **D31** (1985) 17–30.

[29] T. J. Chapin, R. L. Cool, K. A. Goulianos, J. P. Silverman, G. R. Snow, H. Sticker, S. N. White, and Y.-H. Chou, "Development and Performance of a

High Pressure Hydrogen Time Projection Chamber," *Nucl. Instrum. Meth.* **197** (1982) 305.

[30] **MuCap** Collaboration, J. Egger, M. Hildebrandt, and C. Petitjean, "The 10bar hydrogen time projection chamber of the MuCap experiment," *Nucl. Instrum. Meth.* **A628** (2011) 199–203.

[31] P. Baron, E. Delagnes, C. Flouzat, and F. Guilloux, "Dream, a front end asic for clas12 detector user manual." http://userweb.jlab.org/~jixie/bonus12/DREAM_UserManual_prod_v1.pdf.

[32] SRIM, "The stopping and range of ions in matter." http://www.srim.org.

[33] S. Kuhn. Personal communication, 2015.

[34] NIST, "Stopping-power and range tables for electrons, protons, and helium ions." http://physics.nist.gov/PhysRefData/Star/Text/PSTAR-t.html.

[35] **A1** Collaboration, J. C. Bernauer *et al.*, "High-precision determination of the electric and magnetic form factors of the proton," *Phys. Rev. Lett.* **105** (2010) 242001, arXiv:1007.5076 [nucl-ex].

[36] G. G. Simon, C. Schmitt, F. Borkowski, and V. H. Walther, "Absolute electron Proton Cross-Sections at Low Momentum Transfer Measured with a High Pressure Gas Target System," *Nucl. Phys.* **A333** (1980) 381–391.

[37] J. J. Murphy, Y. M. Shin, and D. M. Skopik, "Proton form factor from 0.15 to 0.79 fm-2," *Phys. Rev.* **C9** (1974) 2125–2129. [Erratum: Phys. Rev.C10,2111(1974)].

[38] A. Gasparian *et al.*, "High Precision Measurement of the Proton Charge Radius (A New Proposal to Jefferson Lab PAC-38),". www.jlab.org/exp_prog/proposals/11/PR12-11-106.pdf.

[39] R. Jones, "Hall d coherent bremsstrahlung rate calculator." http://zeus.phys.uconn.edu/halld/cobrems/ratetool.cgi.

[40] **Particle Data Group** Collaboration, K. A. Olive *et al.*, "Review of Particle Physics," *Chin. Phys.* **C38** (2014) 090001.

[41] E. R. Berger, M. Diehl, and B. Pire, "Time - like Compton scattering: Exclusive photoproduction of lepton pairs," *Eur. Phys. J.* **C23** (2002) 675–689, arXiv:hep-ph/0110062 [hep-ph].